Journal of Alloys and Compounds 503 (2010) 96–102

Contents lists available at ScienceDirect

Journal of Alloys and Compounds

journal homepage: www.elsevier.com/locate/jallcom

The interface states and series resistance effects on the forward and reverse bias I–V, C–V and G/ω-V characteristics of Al–TiW–Pd_2Si/n-Si Schottky barrier diodes

H. Uslu [a], Ş. Altındal [a], U. Aydemir [a], İ. Dökme [b,*], İ.M. Afandiyeva [c]

[a] Department of Physics, Gazi University, 06500 Ankara, Turkey
[b] Science Education Department, Gazi Education Faculty, Gazi University, 06500 Ankara, Turkey
[c] Baku State University, Baku, Azerbaijan

ARTICLE INFO

Article history:
Received 19 January 2010
Received in revised form 21 April 2010
Accepted 28 April 2010
Available online 5 May 2010

Keywords:
Al–TiW–Pd_2Si/n-Si Schottky barrier diodes
Illumination effect
Series resistance
Interface states

ABSTRACT

Illumination intensity effects on the electrical characteristics of Al–TiW–Pd_2Si/n-Si Schottky structures have been investigated in this study for the first time. The electrical parameters such as ideality factor (n), zero-bias-barrier height (Φ_{B0}), series resistance (R_s), depletion layer width (W_D) and dopping concentration (N_D) of Al–TiW–Pd_2Si/n-Si Schottky barrier diodes (SBDs) have been investigated by using the forward and reverse bias current–voltage (I–V), capacitance–voltage (C–V) and conductance–voltage (G/ω-V) measurements in dark and under illumination conditions at room temperature. The values of C and G/ω increase with increasing illumination intensity due to the illumination induced electron–hole pairs in the depletion region. The density of interface states (N_{ss}) distribution profiles as a function of ($E_c - E_{ss}$) was extracted from the forward I–V measurements by taking into account the bias dependence of the effective barrier heights (Φ_e) for device in dark and under various illumination intensities. The high values of N_{ss} were responsible for the nonideal behavior of I–V, C–V and G/ω characteristics. The values of R_s obtained from Cheung and Nicollian methods decrease with increasing illumination intensity. The high values of n and R_s have been attributed to the particular distribution of N_{ss}, surface preparation, inhomogeneity of interfacial layer and barrier height at metal/semiconductor (M/S) interface. As a result, the characteristics of SBD are affected not only in N_{ss} but also in R_s, and these two parameters strongly influence the electrical parameters.

© 2010 Elsevier B.V. All rights reserved.

1. Introduction

Aluminum (Al) and palladium silicide (PdSi) have become the most widely used small area rectifier contact onto Si [1–6] instead of platinum silicide (PtSi) in recently [7–9]. Since, PtSi contacts suffer from a number of processing difficulties associated with the Pt due to its high melting temperature. Because of the importance of metal silicide in integrate circuit technology Pd_2Si films on Si have received a lot of attention in the past. The first studies on Pd_2Si films were made by Kircher [4]. He investigated the metallurgical properties and electrical characteristics of Pd_2Si contacts on n-Si. Wittmer et al. [5] and Shepela [6] carry out the measurement of resistivity of Pd_2Si film grown on Si substrate. Knowledge of the electrical characteristics of the silicide at the interfaces is important for understanding the formation of Schottky barriers and interface states between silicide and Si interfaces. The electrical properties of the SBDs depend especially on the R_s of device, the existence of N_{ss} and native or deposited interfacial insulator layer and barrier formation at M/S interface. The analysis of SBDs only in dark cannot give detailed information about structural parameters of devices. On the other hand, the main electrical parameters of SBDs can be strong function of the intensity of illumination level. Since, under illumination, photons whose energy values ($hc/q\lambda$) are grater than the energy band gap of semiconductor (E_g) can generate electron–hole pairs in the depletion region of the semiconductor. Under an external and a native electric field due to electron–hole diffusion at M/S interface, the holes swept to the back contact while electrons gathered at the junction. Also, it has been well known that there are currently many reports on experimental studies of metal–semiconductor (MS) and metal–insulator–semiconductor (MIS) Schottky barrier diodes (SBDs) [10–17]. Consequently, there would be an additional photocurrent over the usual dark diode current [18–20].

In our previous study [2], we reported the experimental results of I–V characteristics of Al–TiW–Pd_2Si/n-Si as a function of temperature. Our another studies [3,21] include the frequency dependence of electrical and dielectrical characteristics of Al–TiW–Pd_2Si/n-Si structures at room temperature. It was found that the R_s and N_{ss} of the Al–TiW–Pd_2Si/n-Si were important parameters that strongly influence the frequency dependent C–V and conductance–voltage

* Corresponding author.
E-mail address: ilbilgedokme@gazi.edu.tr (İ. Dökme).

0925-8388/$ – see front matter © 2010 Elsevier B.V. All rights reserved.
doi:10.1016/j.jallcom.2010.04.210

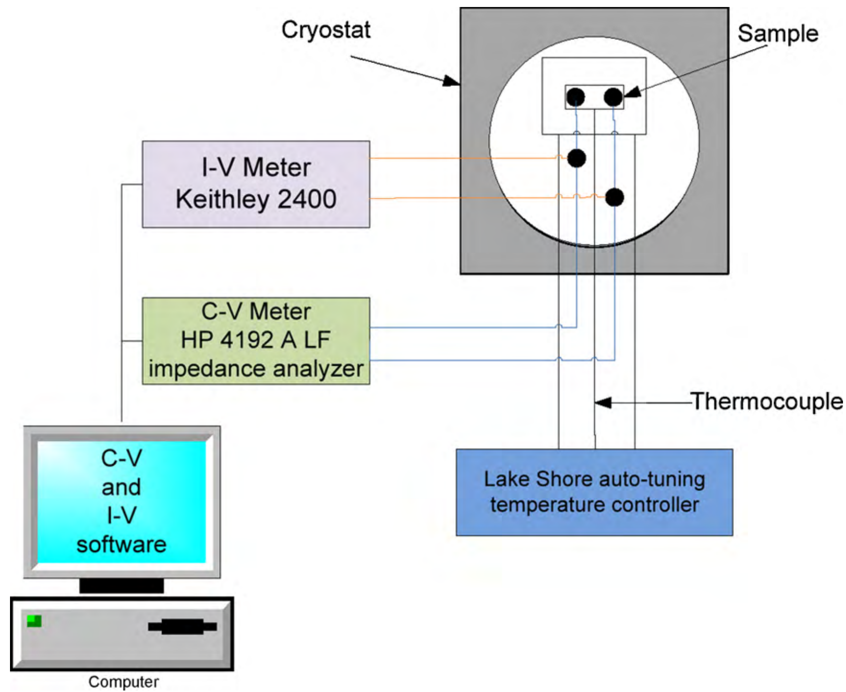

Fig. 1. The schematic diagram of measurement systems.

(G/ω-V) characteristics of device. However, the illumination effect on main these parameters of metal–Pd_2Si/Si structures have not been investigated in detail yet. Therefore, we aimed to investigate the illumination effect on main electrical parameters at various illumination intensities. We found that the effect of illumination approaches to a saturation level of 20 mW/cm^2 approximately. Also, high illumination intensities can cause the sample get warmer.

It is an interest to investigate the illumination effect on main electrical parameters of Al–TiW–Pd_2Si/n-Si SBDs by using I–V, C–V and G/ω-V measurement methods in dark and under illumination conditions. Therefore, the first aim of this study is to investigate the illumination effect on main electrical parameters such as n, Φ_{B0}, W_D and N_D in Al–TiW–Pd_2Si/n-Si SBDs under dark and illumination conditions at room temperature. The second aim is to achieve a better understanding of the effect of R_s and N_{ss} on the I–V, C–V and G/ω-V characteristics in the wide range illumination levels and applied bias voltages.

2. Experimental procedures

The Al–TiW–Pd_2Si/n-Si SBDs were fabricated on 2 in. diameter n-type (P doped) single crystal silicon wafer with (1 1 1) surface orientation, 0.07 Ω cm resistivity and 3.5 μm thickness. The pattern of these structures were formed by a photolithographic technique, and annealed at 773 K for 1 min in flowing dry nitrogen (N_2) ambient in a rapid thermal annealing furnace. Respect to homogeneity, the low area of SBD is an advantage and it is important for the current density and open circuit voltage. In addition, 8×10^{-6} m^2 (=8×10^{-2} cm^2) area is corresponding to 3.2 mm diameter. For the fabrication process, the Si wafer first was cleaned in a mix of a peroxide-ammoniac solution in 10 min and subsequently quenched in de-ionized water of resistivity of 18 MΩ cm for a prolonged time.

In order to form ohmic and rectifier contacts of the sample, we used the BESTEC thermal evaporation system in high vacuum (∼10^{-6} Torr). In deposition chamber, the evaporator has four crucibles made by tungsten to evaporate different metals onto sample. The evaporator provides with a dc power supply (maximum voltage = 8 V and current = 400 A). Also, a thickness meter, substitute near sample, measures the thickness of deposited metal and deposition rate during the evaporation procedure.

After the cleaning process, high purity (99.999%) Al with a thickness of about 2000 Å were thermally evaporated onto whole back side of Si wafer at a pressure about 10^{-6} Torr in high vacuum system. The ohmic contacts were formed by annealing them for a few minutes at 450 K. To fabricate Pd_2Si layer, palladium was deposited on Si wafer by using thermal evaporation method at 250 K. At this temperature, the Pd deposited on the contact regions reacts to form Pd_2Si. The unconverted Pd was etched away with an aqueous solution of KI + I_2, an etchant which does not attack Pd_2Si, and subsequently annealed at 300 K for 15 min. The thickness of Pd_2Si was determined to be about 0.6 μm by the use of the spectroscopic ellipsometry system (Jobin Yvon-Horiba). To form the metal electrodes (rectifier and ohmic contacts), traditionally Al dots could have been formed on Pd_2Si-nSi structure, but Al has high diffusion ability and it can lead to degrade contact's quality. Therefore, in this work, to prevent the disadvantage of Al diffusion to Si, the TiW alloy, played the role of the diffusion barrier between Pd_2Si and Al, was deposited on Pd_2Si–nSi layer. For this process, the sandwiched structure Al–$Ti_{10}W_{90}$ was deposited by the

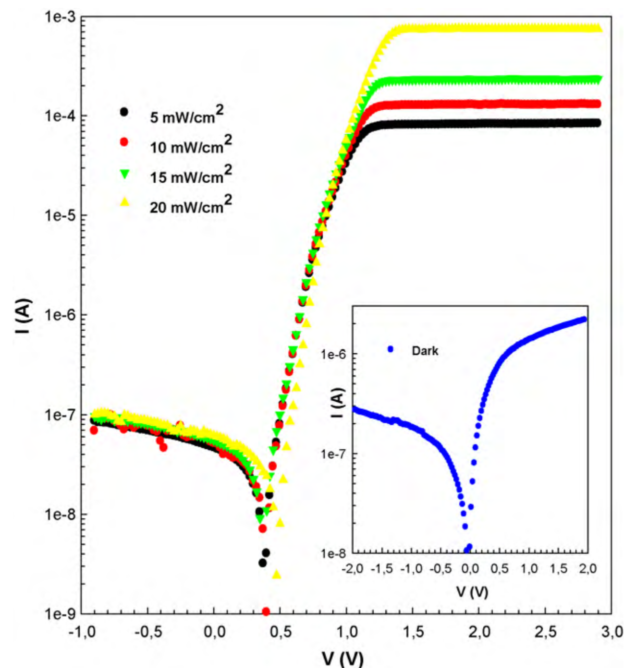

Fig. 2. The forward and reverse bias semi-logarithmic I–V characteristics of Al–TiW–Pd_2Si/n-Si SBD in dark (inset of Fig. 1) and under various illumination intensities at room temperature.

Table 1
Illumination dependent values of various parameters determined from forward bias *I–V* characteristics of Al–TiW–Pd_2Si/*n*-Si SBD at room temperature.

Power (mW/cm^2)	I_0 (A)	n	Φ_{B0} (*I–V*) (eV)	R_s (dV/dln(*I*)) (Ω)	R_s (*H*(*I*)) (Ω)	N_{ss} (eV^{-1}/cm^2)
0	5.40×10^{-8}	5.25	0.701	986481	375104	2.34×10^{14}
5	3.70×10^{-8}	5.46	0.710	1210	2310	2.46×10^{14}
10	2.67×10^{-8}	5.05	0.718	7091	1380	2.23×10^{14}
15	2.19×10^{-8}	4.74	0.723	3490	706	2.06×10^{14}
20	4.27×10^{-9}	3.92	0.764	835	340	1.61×10^{14}

magnetron sputtering method at substrate temperature of 420 K in vacuum system 'Oratoria-5' and then annealed at temperature of 500 K in nitrogen atmosphere (N_2) for 20 min.

Prior to the deposition, vacuum and target conditions were performed. Taking into account the dispersion factor of Ti and W, the compound target (Ti 10%, W 90%) was made. The deposition chamber was pumped down to the ultimate vacuum and repeatedly charged with argon in order to minimize the residual gas components. The alloy compound target film was bombarded by Ar^+ ions with high energy at room temperature. The base pressure during the ion bombardments was about 10^{-6} Torr. Al was also deposited onto TiW–Pd_2Si/*n*-Si structure by the same method until the thickness of Al film on $Ti_{10}W_{90}$–Pd_2Si-*n*Si layer was about 1 μm.

A simple illustration of measurement systems is given in Fig. 1. In dark and under illumination conditions, the forward and reverse bias current–voltage (*I–V*) characteristics of Al–TiW–Pd_2Si/*n*-Si SBDs were performed by the use of a Keithley 220 programmable constant current source together with a Keithley 614 electrometer. The capacitance–voltage (*C–V*) and conductance-voltage (*G*/*ω*-*V*) characteristics of these devices were performed by the use HP4192A-LF impedance analyzer (5 Hz–13 MHz). Small sinusoidal signal of 40 mV peak to peak from the external pulse generator is applied to the sample in order to meet the requirement [22]. All measurements were carried out with the help of a microcomputer through an IEEE-488 ac/dc converter card in a Janis vpf-475 cryostat to prevent out environment conditions. For the illumination of sample, a 250 W solar simulator (Model: 69931, Newport-Oriel Instruments, Stratford, CT, USA) was used as a light source. The photons at different power levels were passed through an AM1.5 filter which allowed wavelengths only between 400 and 700 nm to be incident upon the diodes. The intensity of the light was measured by research radiometer (Model ILT1700, International Light Technologies, Massachusetts, USA) and experiments were carried out 5, 10, 15, 20 mW/cm^2 illumination levels.

3. Results and discussion

3.1. Illumination intensity dependence of the I–V characteristics

For SBDs with a series resistance R_s, the relation between the applied forward bias voltage (V) and the current (I) can be written as [22]:

$$I = I_0 \exp\left(\frac{q(V-IR_s)}{nkT}\right)\left[1-\exp\left(-\frac{q(V-IR_s)}{kT}\right)\right] \quad (1)$$

where I_0 is the reverse saturation current and it can be described as

$$I_0 = AA^*T^2 \exp(-\frac{q\Phi_{B0}}{kT}) \quad (2)$$

where the quantities IR_s, A, A^* (120 A/cm^2 K^2 for n-type Si), T, k and Φ_{B0} are the terms of the voltage drop across series resistance, the rectifier contact area, the effective Richardson constant, temperature in Kelvin, Boltzmann constant and the zero-bias barrier height, respectively. Fig. 2 shows the forward and reverse bias *I–V* characteristics of the Al–TiW–Pd_2Si/*n*-Si SBDs, measured in dark and under various illumination intensities at room temperature. The forward current at high bias region increases with the increasing illumination intensity due to the fact that photons can generate electron–hole pairs in the depletion layer of the semiconductor.

The values of I_0 obtained by extrapolating the linear intermediate bias-voltage region of the ln *I–V* curve to zero applied bias-voltage and the Φ_{B0} values calculated from Eq. (2) were shown in Table 1. As shown in Table 1, the Φ_{B0} and n were found to be a strong function of illumination intensity. The values of Φ_{B0} were found to increase, while the values of n decrease with the increasing illumination level (Φ_{B0} = 0.710 eV and n = 5.46 under 5 mW/cm^2 and Φ_{B0} = 0.764 eV and n = 3.92 under 20 mW/cm^2). The illumination dependence of the Φ_{B0} can be described as

$$\Phi_{B0}(P) = \Phi_{B0} - \alpha P \quad (3)$$

where α is the illumination coefficient of Si band gap and P is the intensity of illumination. The fitting of the $\Phi_{B0}(P)$ yields Φ_{B0} = 0.581 eV and $\alpha = -5.1 \times 10^{-4}$ eV/W. This value of illumination coefficient of the Φ_{B0} was in very close agreement with the temperature coefficient of the Si band gap (-4.73×10^{-4} eV/K). This result indicates that the illumination effect on electrical characteristics of SBDs is very important as well as the effect of temperature and these devices can be used as an optical sensor for optoelectronic application.

The R_s effect on the forward bias *I–V* characteristics is shown in Fig. 2, particularly in the downward curvature of *I–V* curves after about 0.5 V. It is well known the value of R_s decreases with the increasing illumination level due to the charge's being stimulated from the valance band to conductance band; therefore this situation causes the downward curvature in the forward bias *I–V* plots under illumination to shift towards high bias region as shown in Fig. 2. Thus, as it can be seen from Fig. 2, the forward bias *I–V* characteristics under 20 mW/cm^2 of illumination level the downward curvature starts after 1.25 V. This effect reduces the linear region of the forward bias ln *I–V* curves. Therefore, the accuracy of the determination of Φ_{B0} and n becomes poorer. In this case, the values of Φ_{B0} and R_s can be evaluated using a method developed by Cheung and Cheung [23] in the high bias voltage where the ln *I–V* curves are not linear behavior as following equations.

$$\frac{dV}{d(\ln I)} = n\left(\frac{kT}{q}\right) + R_s I \quad (4a)$$

$$H(I) = V - n\frac{kT}{q}\ln\left(\frac{I}{AA^*T^2}\right) = n\Phi_{B0} + R_s I \quad (4b)$$

Fig. 3 shows the experimental d*V*/dln(*I*) vs *I* and *H*(*I*) vs *I* plots of the Al–TiW–Pd_2Si/*n*-Si SBD in dark and under four illumination intensities, respectively, at room temperature. These figures have given a straight line for downward curvature region. Thus, the values of n and R_s have been obtained from the intercept and slope of the d*V*/dln(*I*) vs *I* plots (Fig. 3a) at each illumination level. The plots of *H*(*I*) vs *I* (Fig. 3b) give a straight line with a current axis intercept equal to $n\Phi_{B0}$. The slopes of these plots also provide a second determination of R_s, which can be used to check the consistency of this approach. As function of illumination intensity, the values of R_s obtained from Eqs. 4(a) and 4(b) are also presented in Table 1. As shown in Table 1, the obtained R_s values by different methods are almost in agreement with each other and decrease with the increasing illumination intensity. Similar results have been reported in the literature [18–20,24–26]. The results are consistent with a net reduction in carrier density in the depletion region of device through the introduction of traps and recombination centers associated with illumination effect [27].

The values of n and Φ_e are assumed to be voltage dependent and can be written following equations, respectively [28,29].

$$n(V) = \frac{q}{kT}\left[\frac{(V-IR_s)}{\ln(I/I_0)}\right] = 1 + \frac{\delta}{\varepsilon_i}\left[\frac{\varepsilon_s}{W_D} + qN_{ss}(V)\right] \quad (5)$$

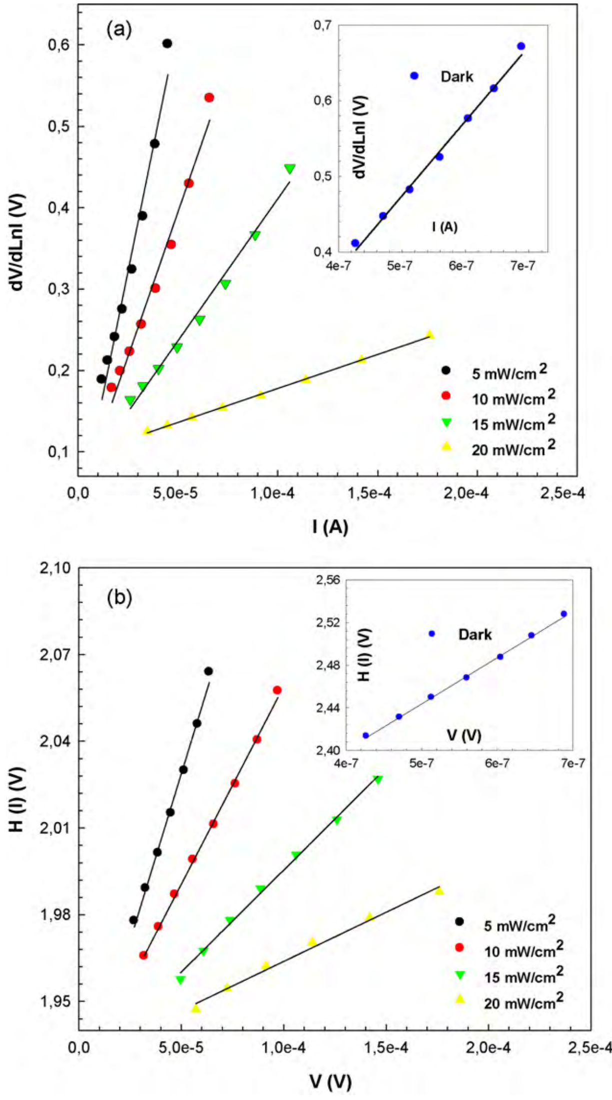

Fig. 3. (a) Experimental $dV/d\ln(I)$ vs I and (b) $H(I)$ vs I plots of Al–TiW–Pd_2Si/n-Si SBD in dark (in and inset of Fig. 2) and under various illumination intensities at room temperature.

$$\Phi_e = \Phi_{B0} + \beta(V - IR_s) = \Phi_{B0} + \left(1 - \frac{1}{n(V)}\right)(V - IR_s) \quad (6)$$

where β is the voltage coefficient of the Φ_e. The expression of Eq. (5) is identical to Eq. (18) of Card and Rhoderick [28] and the expression for the interface state density is reduced to

$$N_{ss}(V) = \frac{1}{q}\left[\frac{\varepsilon_i}{\delta}(n(V) - 1) - \frac{\varepsilon_s}{W_D}\right] \quad (7)$$

where δ is the thickness of interfacial insulator layer, W_D is the depletion layer width, ε_i and ε_s ($\varepsilon_i = 3.8\varepsilon_0$, $\varepsilon_s = 11.8\varepsilon_0$) are permittivity of the interfacial insulator layer and the semiconductor, respectively, and ε_0 is the permittivity of the free space charge. Furthermore in n-type semiconductors, the energy of interface states N_{ss} with respect to the bottom of conduction band E_c at the surface of the semiconductor can be obtained according to refs. [22,24]. The W_D was also calculated C–V characteristic for each illumination intensity at 50 kHz using the equation for the width of the space charge region ($W_D = [2\varepsilon_s\varepsilon_0 V_d/qN_D]^{1/2}$). Furthermore, in n-type semiconductors, the energy of the interface states E_{ss} with respect to the bottom of the conduction band at the surface of semiconductor is given by

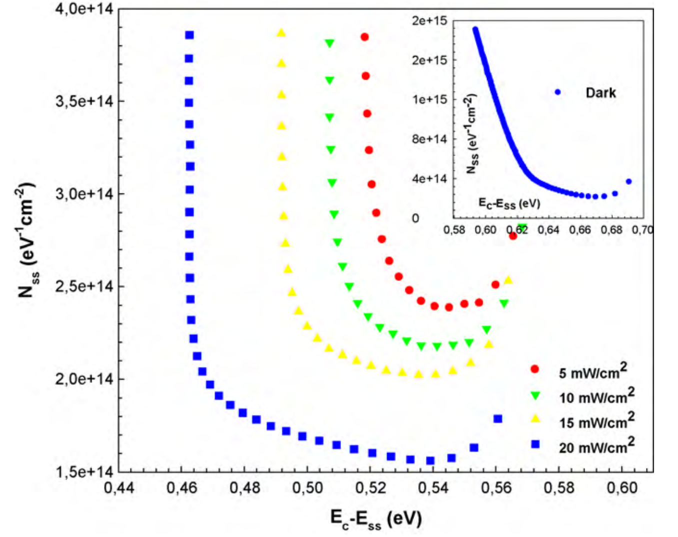

Fig. 4. The energy distribution profile of the N_{ss} obtained from the forward bias I–V characteristics of Al–TiW–Pd_2Si/n-Si SBD in dark (inset of Fig. 3) and under various illumination intensities at room temperature.

$$E_c - E_{ss} = q(\Phi_e - V) \quad (8)$$

Substituting in Eq. (7) the values of the voltage dependence of $n(V)$, δ and W_D, the energy distribution profile of N_{ss} as a function of ($E_c - E_{ss}$) were extracted from the forward bias I–V measurements by taking the bias dependence of the effective BH (Φ_e) into account in dark and under illumination conditions and are given in Fig. 4. As shown in Fig. 4, the exponential growth of the N_{ss} from midgap towards the bottom of conduction band is very apparent. In addition the values of N_{ss} decrease with increasing illumination intensity between the (E_c–0.46) and (E_c–0.56) eV.

Experimental results show that the values of N_{ss} and R_s are very important parameters which cause deviation from the ideality. However, while the values of R_s are significant in the downward curvature of the forward bias I–V characteristics, but the values of N_{ss} are effective in all forward bias region and their distribution changes from region to region in the bandgap of semiconductor at metal–semiconductor interface.

The values of R_s and Φ_B were obtained from the modified Norde method developed by Bohlin [30]. While Cheung's functions are only executed for the nonlinear region of the forward bias I–V plots, Norde's functions are executed for the whole forward bias region of I–V plots of the SBDs. The R_s values from the modified Norde and Cheung and Cheung methods have been compared with each other. The modified Norde method is expressed as

$$F(V, \gamma) = \frac{V}{\gamma} - \frac{q}{kT}\ln\left(\frac{I}{AA^*T^2}\right) \quad (9)$$

where γ is the dimensionless value greater than ideality factor. According this method, once the minimum of the $F(V, \gamma)$ vs V plot is determined, the value of Φ_B and R_s can be obtained from following equations, respectively.

$$\Phi_B = F(V_0) + \frac{V_0}{\gamma} - \frac{kT}{q} \quad (10a)$$

$$R_s = \left(\frac{kT}{qI}\right)(\gamma - n) \quad (10b)$$

where $F(V_0)$ is the minimum point of $F(V, \gamma)$ vs V plot, V_0 and I are the corresponding bias voltage and current, respectively. Fig. 5 shows the $F(V)$ vs V plots for the Al–TiW–Pd_2Si/n-Si SBDs. The values of Φ_B and R_s obtained from Eqs. (10a) and (10b) in dark and under various

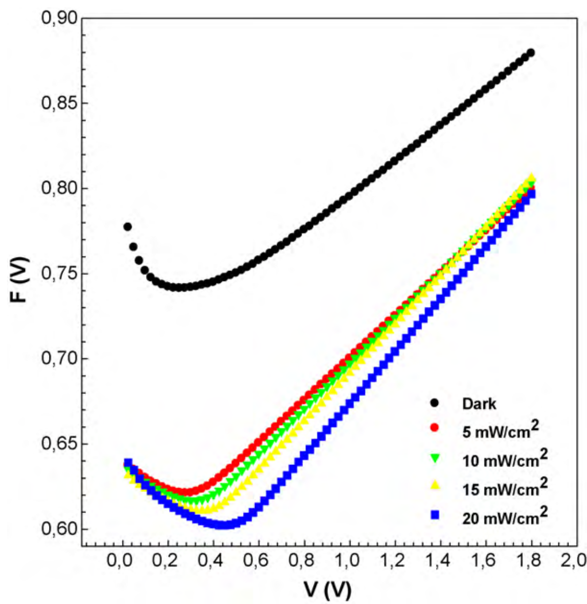

Fig. 5. The $F(V)$ vs V plots for the Al–TiW–Pd_2Si/n-Si SBD in dark and under various illumination intensities at room temperature.

illumination conditions are given in Table 2. As shown in Table 2, the Φ_B and R_s were found to be a strong function of illumination intensity. The values of R_s and Φ_B decrease with the increasing illumination intensity. Similar change of R_s and Φ_B values calculated from Cheung and Cheung [23] method is seen in Table 1. The R_s values were found as 236 kΩ in dark and 0.146 kΩ under illumination (20 mW/cm^2).

3.2. Illumination intensity dependence of the C–V and G/ω-V characteristics

In the high and intermediate frequency range, the effect of N_{ss} can be ignored. Also, at high frequency the effect of R_s becomes important and a correction in the C–V and G/ω-V plots is required for the effect of R_s. However at low and intermediate frequency the effect of R_s can be ignored and it does not give a curvature or peak in the C–V plots in accumulation region. While the value of R_s is effective only in the accumulation region, the value of N_{ss} is effective both in depletion and reverse bias region. Therefore, in the dark and under illumination conditions, the reverse and forward bias C–V and G/ω-V characteristics of Al–TiW–Pd_2Si/n-Si SBD have been measured at room temperature at 50 kHz frequency and are given in Fig. 6(a) and (b), respectively. The C and G/ω values vary from the strong inversion region (−2 V) to the strong accumulation region (4 V). These changes in C and G/ω occur especially in the depletion and accumulation regions while the values of C and G/ω remain almost constant in the inversion region.

In recent years, several methods have been suggested to determine the series resistance of metal–semiconductor (MS) contacts and metal–insulator–semiconductor (MIS) type SBDs [23,31,32]. According to a method presented by Nicollian and Brews [32], the real series resistance of the MS and MIS structures can be calculated from the C and G in strong accumulation region at efficiently high frequencies [32] as

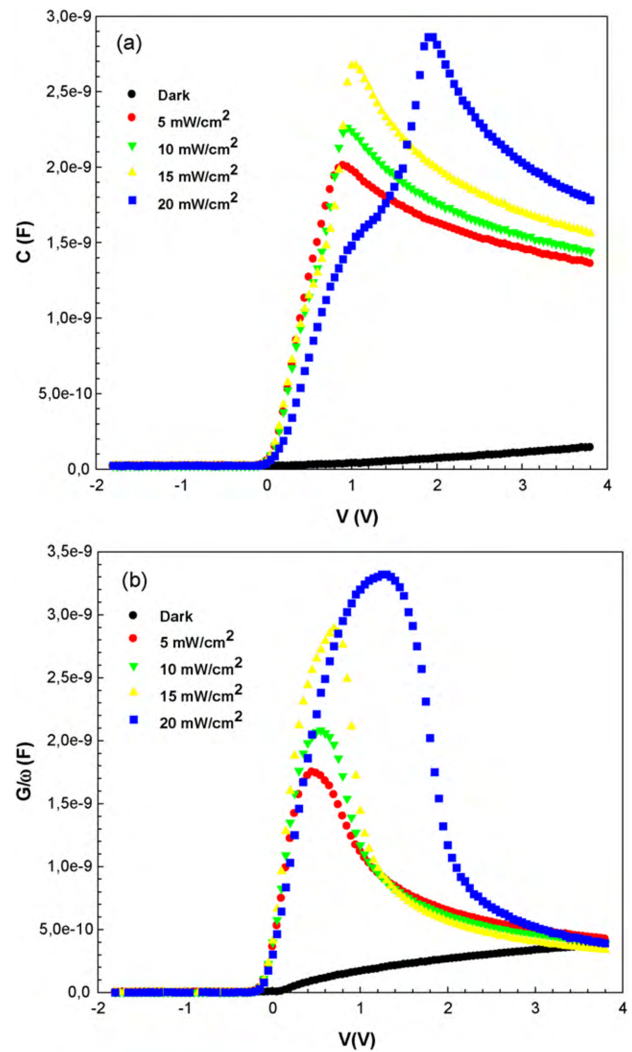

Fig. 6. (a) Measured capacitance C vs V and (b) conductance G/ω vs V plots of Al–TiW–Pd_2Si/n-Si SBD in dark and under various illumination intensities.

$$R_s = \frac{G}{G^2 + (\omega C)^2} \quad (11)$$

As seen in Fig. 6(a), the measured capacitance gives a peak between about 0.9–1.95 V depending on illumination intensity and disappears in the dark condition. Also, the peak magnitude increases with the increasing illumination intensity and shifts toward positive bias voltage. These behaviors are considered that the trap charges have enough energy to escape from the traps located at M/S interface in the Si band gap due to illumination effect. The G/ω-V characteristics are parallel with the C–V characteristics in the same bias range. Such behavior of C–V and G/ω-V characteristics may be

Table 2
Illumination dependent values of various parameters determined from the modified Norde function for Al–TiW–Pd_2Si/n-Si SBD.

Power (mW/cm^2)	V_0 (V)	I (A)	$F(V_0)$ (V)	Φ_B (eV)	R_s (Ω)
0	0.25	3.44×10^{-7}	0.741	0.746	2.36×10^5
5	0.27	5.14×10^{-5}	0.621	0.630	1.23×10^3
10	0.30	7.65×10^{-5}	0.617	0.632	8.02×10^2
15	0.35	1.46×10^{-4}	0.611	0.636	3.87×10^2
20	0.45	4.41×10^{-4}	0.602	0.647	1.46×10^2

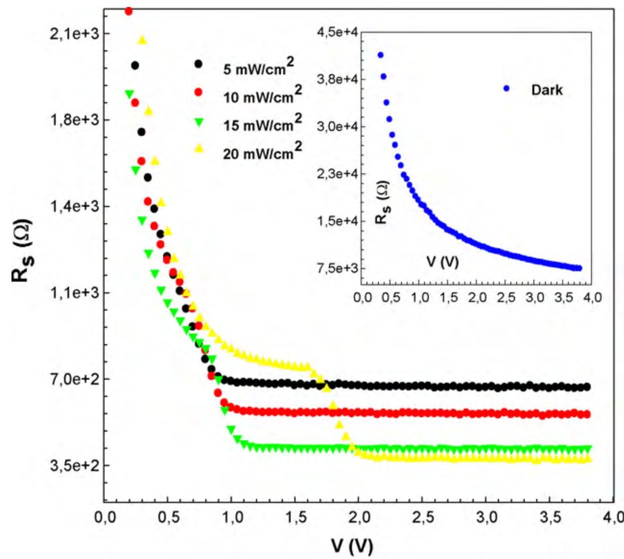

Fig. 7. The series resistance profile of Al–TiW–Pd_2Si/*n*-Si SBD calculated from measured capacitance *C* and conductance G/ω data in dark (Fig. 6 (a and b)) and under various illumination intensities.

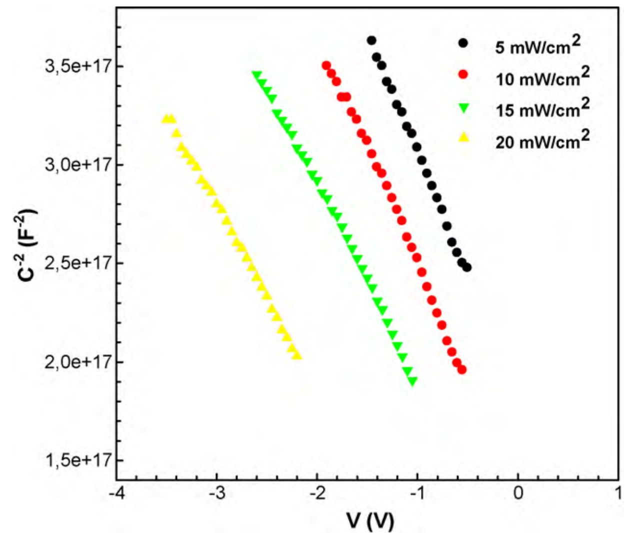

Fig. 8. The reverse bias C^{-2}–V characteristics of Al–TiW–Pd_2Si/*n*-Si SBD under various illumination intensities at 50 kHz and room temperature.

attributed to particular distribution of N_{ss}. It is well known, for a Schottky barrier diode 2 V is sufficiently large especially for the forward *I*–*V* measurements. Almost all changes in the main electrical parameters arise from at low bias region. As mention above at high bias voltage the value of R_s becomes very effective on the *C*–*V* characteristics especially at high forward biases and leads to a concave curvature in these plots.

The values of R_s have been calculated according to Eq. (11) in dark and under various illumination intensities (Fig. 7). These very significant values demanded that special attention be given to effects of the series resistance in the application of the admittance-based measured methods (*C*–*V* and G/ω-*V*). It can be seen in Fig. 7, the values of R_s in the depletion and accumulation regions decrease with the increasing illumination intensities.

In order to assess the N_D, W_D, Φ_B and N_{ss} values, the C^{-2} vs *V* plots have been obtained from the reverse bias *C*–*V* data, given in Fig. 8 for various illumination intensities at room temperature. The *C*–*V* relationship for the MS and MIS type SBDs can be written as [22].

$$C^{-2} = \frac{2(V_R + V_0)}{q\varepsilon_s\varepsilon_0 A^2 N_D} \tag{12a}$$

$$\frac{d\left(C^{-2}\right)}{dV} = \frac{2}{q\varepsilon_s\varepsilon_0 A^2 N_D} \tag{12b}$$

where V_0 and N_D are intercept voltage and doping concentration, respectively. The values of V_0 were determined from the extrapolation of the linear part of C^{-2} vs *V* (Fig. 8) plot to voltage axis, while the values of N_D were calculated from slope of the same plot at 50 kHz. Thus, the Φ_B can be expressed as

$$\Phi_B(C-V) = V_0 + \frac{kT}{q} + E_F - \Delta\Phi_B = V_D + E_F - \Delta\Phi_B \tag{13}$$

where V_D is the diffusion potential and $\Delta\Phi_B$ is the image force barrier lowering and given by [22],

$$\Delta\Phi_B = \sqrt{\frac{qE_m}{4\pi\varepsilon_s\varepsilon_0}} \tag{14}$$

where $E_m = \sqrt{2qN_D V_D/\varepsilon_s\varepsilon_0}$ is the maximum electric field. The Fermi energy level (E_F) values can be obtained as [22],

$$E_F = \frac{kT}{q}\ln\left(\frac{N_c}{N_D}\right) \tag{15a}$$

with

$$N_c = 4.82 \times 10^{15} T^{3/2}\left(\frac{m_e^*}{m_0}\right)^{3/2} \tag{15b}$$

where N_c is the effective density of states in Si conductance band and $m_0 = 9.1 \times 10^{-31}$ kg the rest mass of the electron. The variation of the N_D, W_D and Φ_B values obtained from the C^{-2} vs *V* characteristics for various illumination intensities are shown in Table 3. As shown in Table 3, the values of N_D, W_D and Φ_B were a strong function of illumination intensity. The W_D and Φ_B values were found to decrease, while the N_D increases with the increasing illumination intensity. These changes related to values of capacitance dependence on illumination intensity (Fig. 6a). Such behavior of *C* may be attributed to the shrinking of the depletion region width (W_D) and restructure and reordering of interface states under illumination effect.

The relationship of theoretical carrier doping concentration $N'_D = 6.16 \times 10^{16}$ cm^{-3} and the experimental carrier doping concentration N_D is given by [33–35]

$$c_2 = -\frac{2}{q\varepsilon_s\varepsilon_0 N_D\left(d\left(C^{-2}\right)/dV\right)} \cong \frac{N_D}{N'_D} = \frac{\varepsilon_i}{\varepsilon_i + q\delta N_{ss}} = \frac{1}{n} \tag{16}$$

The values of N_{ss} given in Table 3 have been calculated at various illumination intensities by using Eq. (16). It is clear that the

Table 3
Illumination dependent values of various electrical parameters obtained from reverse bias C^{-2}–V characteristics of Al–TiW–Pd_2Si/*n*-Si SBD.

Power (mW/cm^2)	V_D (V)	N_D (cm^{-3})	E_F (eV)	$\Delta\Phi_B$ (meV)	W_D (cm)	Φ_B (eV)	N_{ss} (eV^{-1}/cm^2)	c_2	$n = 1/c_2$
5	1.10	1.80×10^{16}	0.184	30.82	2.83×10^{-5}	1.15	2.70×10^{13}	0.29	3.43
10	0.95	1.89×10^{16}	0.182	30.10	2.56×10^{-5}	1.10	2.51×10^{13}	0.31	3.25
15	0.55	2.24×10^{16}	0.178	27.37	1.79×10^{-5}	0.70	1.95×10^{13}	0.36	2.75
20	0.30	2.33×10^{16}	0.177	23.76	1.30×10^{-5}	0.47	1.83×10^{13}	0.38	2.64

value of N_{ss} decreases with the increasing illumination intensity. Such behavior of N_{ss} may be explained by charge and discharge of interface states under illumination effect.

4. Conclusions

The forward and reverse bias *I–V*, *C–V* and *G/ω-V* characteristics of Al–TiW–Pd_2Si/*n*-Si SBDs have been investigated in the dark and under various illumination conditions at room temperature. Experimental results show that the main electrical parameters such as the n, Φ_{B0}, R_s, W_D, N_D and N_{ss} values were found to depend on the illumination intensity strongly. The values of R_s have been obtained from three methods: Cheung, Bohlin and Nicollian methods. It was found that the R_s values from these methods are in agreement with each other. The high values of n and R_s were attributed to the existence of inhomogeneity of the interfacial layer and the barrier height at M/S interface, particular distribution of N_{ss} in Si band gap and surface preparation. The energy distribution profile of N_{ss} was determined from the forward bias *I–V* characteristics by taking the bias dependence of the effective barrier height (Φ_e) into account and decrease with the increasing illumination intensity. The values of c_2, obtained from the C^{-2} vs V characteristics, are sufficiently smaller than unity. These small values of c_2 were attributed to the order of the magnitude high density of N_{ss} at M/S interface. The values of W_D and barrier height (Φ_B) obtained from reverse bias *C–V* characteristics were found to decrease, while the N_D increases with the increasing illumination intensity. As a result, the electrical characteristics of Al–TiW–Pd_2Si/*n*-Si SBDs are affected not only in N_{ss} but also in R_s.

References

[1] C.K. Tan, A.A. Aziz, F.K. Yam, C.W. Lim, Z. Hassan, A.Y. Hudeish, Funct. Mater. Dev. 517 (2006) 242.
[2] İ. Dökme, Ş. Altındal, İ.M. Afandiyeva, Semicond. Sci. Technol. 23 (2008) 035003.
[3] İ.M. Afandiyeva, İ. Dökme, Ş. Altındal, L.K. Abdullayeva, Sh.G. Askerov, Microelectron. Eng. 85 (2008) 365.
[4] C.J. Kircher, Solid State Electron. 14 (1971) 507.
[5] M. Wittmer, D.L. Smith, P.W. Lew, M.A. Nicolet, Solid State Electron. 21 (1978) 573.
[6] A. Shepela, Solid State Electron. 16 (1973) 477.
[7] D. Dwivedi, R. Dwivedi, S.K. Srivastava, Microelectron. J. 29 (1998) 445.
[8] A. Sellai, Z. Quennoughi, Mater. Sci. Eng. B 155 (2008) 179.
[9] E. Alptekin, M.C. Ozturk, V. Misra, IEEE Electron Dev. Lett. 30 (2009) 331.
[10] A. Tataroğlu, Ş. Altındal, J. Alloys Compd. 484 (2009) 405.
[11] A. Tataroğlu, Ş. Altındal, J. Alloys Compd. 479 (2009) 893.
[12] K. Ejderha, N. Yıldırım, B. Abay, A. Turut, J. Alloys Compd. 484 (2009) 870.
[13] G. Güler, S. Karataş, Ö. Güllü, Ö.F. Bakkaloğlu, J. Alloys Compd. 486 (2009) 343.
[14] A.A.M. Farag, A. Ashery, E.M.A. Ahmed, M.A. Salem, J. Alloys Compd. 495 (2010) 116.
[15] V. Janardhanam, A.A. Kumar, V.R. Reddy, P.N. Reddy, J. Alloys Compd. 485 (2009) 467.
[16] A.A.M. Farag, F.S. Terra, G.M. Mahmoud, A.M. Mansour, J. Alloys Compd. 481 (2009) 427.
[17] Ş. Aydoğan, K. Çınar, H. Asıl, C. Çoşkun, A. Türüt, J. Alloys Compd. 476 (2009) 913.
[18] A.A.M. Farag, I.S. Yahia, M. Fadel, Int. J. Hydrogen Energy 34 (2009) 4906.
[19] F. Yakuphanoğlu, J. Alloys Compd. 494 (2010) 451.
[20] B. Akkal, Z. Benamara, N.B. Bouiadjra, S. Tizi, B. Gruzza, Appl. Surf. Sci. 253 (2006) 1065.
[21] İ.M. Afandiyeva, İ. Dökme, Ş. Altındal, M.M. Bülbül, A. Tataroğlu, Microelectron. Eng. 85 (2008) 247.
[22] S.M. Sze, Physics of Semiconductor Devices, third ed., John Wiley & Sons, New York, 2007.
[23] S.K. Cheung, N.W. Cheung, Appl. Phys. Lett. 49 (1986) 85.
[24] Ö. Tüzün, Ş. Altındal, Ş. Oktik, Renew. Energy 33 (2008) 286.
[25] F. Yakuphanoğlu, Phys. B: Condens. Matter 389 (2007) 306.
[26] K. Akkılıç, F. Yakuphanoğlu, Microelectron. Eng. 85 (2008) 1826.
[27] M.Y. Feteha, M. Soliman, N.G. Gomaa, M. Ashry, Renew. Energy 26 (2002) 113.
[28] H.C. Card, E.H. Rhoderick, J. Phys. D 4 (1971) 1589.
[29] H. Kanbur, Ş. Altındal, A. Tataroğlu, Appl. Surf. Sci. 252 (2005) 1732.
[30] K.E. Bohlin, J. Appl. Phys. 60 (1986) 1223.
[31] H. Norde, J. Appl. Phys. 50 (1979) 5052.
[32] E.H. Nicollian, J.R. Brews, MOS Physics and Technology, Wiley, New York, 1982.
[33] P. Chattopadhyay, A.N. Daw, Solid State Electron. 29 (1986) 555.
[34] A. Tataroğlu, Ş. Altındal, M.M. Bülbül, Microelectron. Eng. 81 (2005) 140.
[35] A. Singh, Solid State Electron. 28 (1985) 223.